
An Evaluation of Myocardial Fatty Acid and Glucose Uptake Using PET with [¹⁸F]Fluoro-6-Thia-Heptadecanoic Acid and [¹⁸F]FDG in Patients with Congestive Heart Failure

Michael Taylor, Thomas R. Wallhaus, Timothy R. DeGrado, Douglas C. Russell, Peter Stanko, Robert J. Nickles, and Charles K. Stone

William S. Middleton Memorial Veterans Hospital, Madison; Departments of Medical Physics and Medicine, University of Wisconsin-Madison, Madison, Wisconsin; and Department of Medical Physics, Duke University, Durham, North Carolina

Understanding the metabolic consequences of heart failure is important in evaluating potential mechanisms for disease progression and assessing targets for therapies designed to improve myocardial metabolism in patients with heart failure. PET is uniquely suited to noninvasively evaluate myocardial metabolism. In this study, we investigated the kinetics of 14(*R,S*)-[¹⁸F]fluoro-6-thia-heptadecanoic acid (FTHA) and [¹⁸F]FDG in patients with stable New York Heart Association functional class III congestive heart failure and a left ventricular ejection fraction of no more than 35%. **Methods:** Twelve fasting patients underwent dynamic PET studies using [¹⁸F]FTHA and FDG. From the dynamic image data, the fractional uptake rates (*K_i*) were determined for [¹⁸F]FTHA and FDG. Subsequently, serum free fatty acid and glucose concentrations were used to calculate the myocardial free fatty acid and glucose uptake rates, respectively. Uptake rates were compared with reported values for [¹⁸F]FTHA and FDG in subjects with normal left ventricular function. **Results:** The average *K_i* for [¹⁸F]FTHA was 19.7 ± 9.3 mL/100 g/min (range, 7.2–36.0 mL/100 g/min). The average myocardial fatty acid use was 19.3 ± 2.3 mmol/100 g/min. The average *K_i* for FDG was 1.5 ± 0.37 mL/100 g/min (range, 0.1–3.3 mL/100 g/min), and the average myocardial glucose use was 12.3 ± 2.3 mmol/100 g/min. **Conclusion:** Myocardial free fatty acid and glucose use in heart failure can be quantitatively assessed using PET with [¹⁸F]FTHA and FDG. Myocardial fatty acid uptake rates in heart failure are higher than expected for the normal heart, whereas myocardial glucose uptake rates are lower. This shift in myocardial substrate use may be an indication of impaired energy efficiency in the failing heart, providing a target for therapies directed at improving myocardial energy efficiency.

Key Words: PET; myocardial metabolism; 14(*R,S*)-[¹⁸F]fluoro-6-thia-heptadecanoic acid

J Nucl Med 2001; 42:55–62

Congestive heart failure is a progressive disorder characterized by a gradual deterioration of left ventricular function, often in the absence of any definable cardiac events. The mechanisms involved in the progression of heart failure are not well understood but are believed to be, in part, related to alterations in myocardial energy metabolism. Increased adrenergic tone in the setting of heart failure (1) not only exerts a direct toxic effect on the myocyte (2) but also causes unfavorable changes in myocardial energy use (3–5). Increased wall stress and oxygen demand result in increased myocardial oxygen consumption in heart failure (6). At the same time, myocardial energy efficiency is reduced, with wasteful cycling of free fatty acids through lipolysis and re-esterification and suppression of the more energy-efficient metabolism of glucose (5,7).

The purpose of this study was to noninvasively evaluate alterations in myocardial fatty acid and glucose metabolism in nonischemic myocardial segments of patients with stable New York Heart Association functional class III heart failure and dilated cardiomyopathy. We used PET and a novel metabolic tracer, 14(*R,S*)-[¹⁸F]fluoro-6-thia-heptadecanoic acid (FTHA), to assess myocardial fatty acid use and [¹⁸F]FDG to assess myocardial glucose use. We hypothesized that free fatty acid uptake would be increased and glucose uptake suppressed in patients with heart failure. Enhanced [¹⁸F]FTHA uptake reflective of increased fatty acid metabolism and low FDG uptake reflective of reduced glucose metabolism would support the hypothesis that substrate-specific alterations occur in myocardial metabolism in the setting of heart failure.

MATERIALS AND METHODS

Patient Population

This study was reviewed and approved by the human subjects committees at the University of Wisconsin-Madison and William S. Middleton Memorial Veterans Hospital. Twelve patients were recruited from the University of Wisconsin Hospital and Clinics

Received Jan. 28, 2000; revision accepted Jun. 20, 2000.

For correspondence or reprints contact: Thomas R. Wallhaus, MD, Cardiology Section, Department of Medicine, University of Wisconsin Hospital and Clinics, 600 Highland Ave. H6/349, Madison, WI 53792-3248.

TABLE 1
Patient Characteristics

Characteristic	Value
Mean age \pm SEM (y)	64 \pm 14
Cause of heart failure (ischemic/nonischemic)	10 patients/2 patients
Mean rate pressure product \pm SEM (bpm and mm Hg)	9,180 \pm 459
Patients taking ACE inhibitor (%)	91.7 (11/12)
Patients taking digoxin (%)	91.7 (11/12)
Patients taking cholesterol-lowering agent (%)	50 (6/12)
Mean left ventricular ejection fraction \pm SEM (%)	24.4 \pm 2.1

ACE = angiotensin-converting enzyme.

and the William S. Middleton Memorial Veterans Hospital (Table 1). All patients gave informed consent. The patients had a left ventricular ejection fraction of no more than 35% and stable New York Heart Association functional class III congestive heart failure at least 3 mo before the study. Active treatment with an angiotensin-converting enzyme inhibitor (if tolerated) and digitalis (unless contraindicated) were required. No patient was taking β -adreno-receptor blocking agents at the time of the study. Exclusion criteria included a history of diabetes, severe or unstable angina, recent myocardial infarction (<3 mo), and active alcohol or drug abuse.

[¹⁸F]FTHA Production

Nucleophilic aqueous [¹⁸F]fluoride was produced using the 11.4-MeV, 6- to 8-mm proton (only) beam, full width at half maximum, from the RDS 112 cyclotron (CTI, Knoxville, TN) and the high-pressure gold-silver or silver body [¹⁸O]H₂O targets described in detail elsewhere (8). [¹⁸F]FTHA was synthesized through an aminopolyether-supported S_N2 nucleophilic substitution reaction using the tosylated precursor 14(*R,S*)-tosyloxy-6-thiaheptadecanoate (9). [¹⁸F]FTHA was purified by reverse-phase high-performance liquid tomography (HPLC) on a 250 \times 4.6 mm C-18 column (Alltech, Deerfield, IL) using a methanol:water:acetic acid (88:2:0.4) mobile phase at a flow rate of 5 mL/min. The eluent was diluted 1:1 with sterile water and loaded onto a C₁₈ SepPak (Waters, Milford, MA). The SepPak was eluted with 2 mL sterile ethanol. After the ethanol was evaporated, [¹⁸F]FTHA was dissolved in 35 mL 3% human serum albumin. The final product was passed through a 0.22-mm filter (Millipore, Bedford, MA) for

injection. Radiochemical purity was analyzed by reverse-phase HPLC with an analytical C-18 column (Alltech; 3 μ m, 150 \times 4.6 mm). Radioanalytic thin-layer chromatography was used to confirm radiochemical purity using silica plates and the mobile-phase 70:30:1 hexane:ethyl acetate:acetic acid.

FDG Production

FDG was produced using a microwave cavity-based adaptation of the Hamacher synthesis using the 1,3,4,6,-tetra-*O*-acetyl-2-*O*-trifluoromethanesulfonyl- β -D-mannopyranose (mannose triflate) precursor (10). The radiochemical purity of the final product was determined by HPLC using an NH₂ column (Alltech; 10 μ m, 250 \times 4.6 mm, 80:20 acetonitrile:H₂O, 2.0 mL/min). Radioanalytic thin-layer chromatography was used to quantitate [¹⁸F]fluoride in the final preparation (silica plates, 80:20 acetonitrile:H₂O).

PET Procedure

For this study, patients completed an [¹⁸F]FTHA and FDG PET scan on consecutive days under identical conditions (Fig. 1). After an overnight fast (9–14 h), patients gave a brief history and underwent physical examination. Intravenous access was obtained with 20-gauge Angiocath cannulae (BD Infusion Therapy Systems, Sandy, UT) placed in the dorsum of the right hand and the left antecubital fossa. Sequential arterialized venous blood samples were drawn from the right hand, which was in a hand warmer, for the determination of serum glucose and free fatty acid concentrations at the beginning, midpoint, and completion of PET scanning. Serum catecholamine samples were drawn just before PET scanning, with patients supine after 30 min of resting. Serum blood samples were stored at -70°C until analyzed. Patients were positioned supine in the Advance PET scanner (General Electric Medical Systems, Milwaukee, WI) for a whole-body tomograph using a 15.6-cm axial field of view, 35 slices, and 3.8-mm in-plane resolution. After optimization of subject positioning for visualization of the entire heart, transmission scanning was performed for 15 min using three rotating ⁶⁸Ge pin sources.

For the [¹⁸F]FTHA scans, patients received a programmed infusion of 92.5 MBq [¹⁸F]FTHA during 10 min from a syringe pump (Harvard, Cambridge, MA) using a standard 10-mL disposable syringe. For the FDG scans, patients received a 370-MBq bolus infusion of FDG. Dynamic imaging for both studies was performed with a frame rate of 2 min for five scans, 5 min for six scans, and 10 min for one scan. After injection of tracer, approximately 2 mL arterialized venous blood was drawn from the heated-hand intravenous catheter to measure ¹⁸F activity every 2 min for the first 20 min and every 5 min for the last 40 min of the scanning procedure. The samples were then placed on ice and

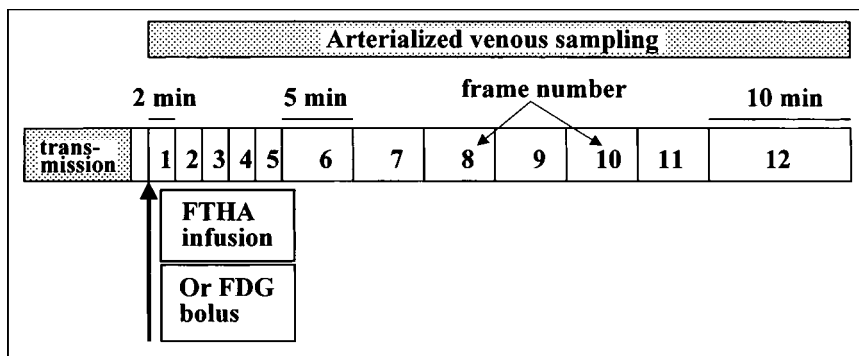


FIGURE 1. Schematic of imaging protocol. FDG was administered as bolus injection, whereas [¹⁸F]FTHA was administered as infusion.

centrifuged. Standard aliquots of plasma were used to determine the time course of radioactivity concentration.

Biochemical Analysis

Norepinephrine and epinephrine levels were determined by high-pressure liquid chromatography with electrochemical detection. Nonesterified free fatty acid levels were measured by spectrophotometric enzymatic assay (Wako Chemicals, USA, Inc., Richmond, VA). Plasma glucose levels were measured by a glucose oxidation assay (CX3-Delta Analyzer; Beckman Instruments, Inc., Brea, CA).

Region-of-Interest Definition

For determination of myocardial radioactivity, or C_i , elliptical regions of interest were drawn within the myocardial border in three contiguous midventricular transaxial slices of each patient within nonischemic myocardial segments showing preserved contractility by echocardiography. PET myocardial transaxial slices were matched with apical long-axis echocardiographic wall segments to assess resting wall motion.

Data Analysis

Myocardial substrate uptake rates from the PET time course data were estimated by graphic analysis (11). The myocardial uptake rates, or K_i , for [^{18}F]FTHA and FDG were first estimated from the relation:

$$\frac{C_i(T)}{C_p(T)} = K_i \frac{\int_0^T C_p dt}{C_p(T)} + V_d$$

where C_i is the myocardial radioactivity and C_p is the plasma [^{18}F]FTHA or FDG radioactivity concentration at time T . Plots of $C_i(T)/C_p(T)$ versus $\int C_p(T)dt/C_p(T)$ were fitted to straight lines by conventional least squares methods, and the slopes of the best-fit lines were taken as estimates of K_i . For the FDG studies, K_i was calculated using the last five dynamic image frames and an uncorrected C_p . For the [^{18}F]FTHA studies, three methods of calculating C_p were evaluated. First, in a subset of five patients, the input function was corrected using the HPLC-determined metabolized fraction. Second, C_p was calculated using data uncorrected for [^{18}F]FTHA metabolites acquired during tracer infusion. Third, a generalized metabolite correction was calculated using the HPLC-corrected data applied to the input function for each patient. K_i values calculated using these three methods were compared. No significant difference was found between K_i values using these three methods of measuring C_p . Consequently, the data taken during the infusion were used to calculate the mean K_i value. The myocardial metabolic uptake rates (MURs) for each region of interest were then calculated from the K_i values by the formula:

$$\text{MUR} = \frac{PK_i}{LC}$$

where P is the plasma glucose or free fatty acid concentration and LC is the lumped constant. The mean serum fatty acid and glucose values obtained during PET were used for determination of P . A lumped constant of 0.67 was assumed for FDG (12), and 1.0 was assumed for [^{18}F]FTHA (13).

Statistical Analysis

Patients' clinical and laboratory data are presented as mean \pm SD. Uptake rate data are presented as mean \pm SEM. The statistical difference between MUR data in this study and MUR data previ-

ously reported in the literature for healthy humans (14,15) was tested using an unpaired Student t test. $P < 0.05$ was considered statistically significant.

RESULTS

Patient Characteristics

Two men with nonischemic cardiomyopathy and 10 men with ischemic cardiomyopathy were recruited. The mean left ventricular ejection fraction was $25\% \pm 6\%$. The medical therapy of all patients remained unchanged for the 3 mo before PET. The patients were receiving standard heart failure medications including angiotensin-converting enzyme inhibitors (92%), digoxin (92%), and diuretics (92%). Six patients (50%) were receiving hydroxymethylglutaryl coenzyme A reductase inhibitors, and one (8%) was receiving gemfibrozil. One patient was receiving an angiotensin II receptor blocking agent (8%). No patients were receiving β -adrenoreceptor blocking agents before PET.

Biochemical Data

Mean serum glucose, free fatty acid, and catecholamine concentrations for patients during [^{18}F]FTHA and FDG scanning are shown in Table 2. No significant differences in mean serum glucose or free fatty acid levels were seen during [^{18}F]FTHA and FDG scanning, suggesting similar metabolic conditions during the procedures. The mean serum catecholamine concentrations were within the normal range of 123–671 pg/mL. Mean serum free fatty acid levels were significantly elevated (1.01 ± 0.08 mmol/L [normal range, 0.40–0.66 mmol/L]) (16). The mean glucose concentration was normal (5.5 ± 0.3 mmol/L [normal range, 3.9–6.1 mmol/L]).

PET Images and Kinetic Analysis for [^{18}F]FTHA

[^{18}F]FTHA uptake was seen in the heart within 90 s after the start of the infusion and provided excellent delineation of myocardial borders. Representative summed short-axis myocardial images at the midventricular level from one patient are shown in Figure 2. A large inferolateral matched metabolic defect is seen on both [^{18}F]FTHA and FDG images. Using data from regions of interest in three consecutive slices, a typical time-activity curve for [^{18}F]FTHA from one patient is shown in Figure 3. The curve shows the

TABLE 2
Laboratory Values

Parameter	FDG scan	[^{18}F]FTHA scan	P
Serum glucose (mmol/L)	5.6 ± 0.3	5.2 ± 0.4	0.39
Serum free fatty acid (mmol/L)	1.01 ± 0.08	0.93 ± 0.06	0.20
Serum catecholamine (pg/mL)	480 ± 40	470 ± 77	0.41

Values are mean \pm SEM.

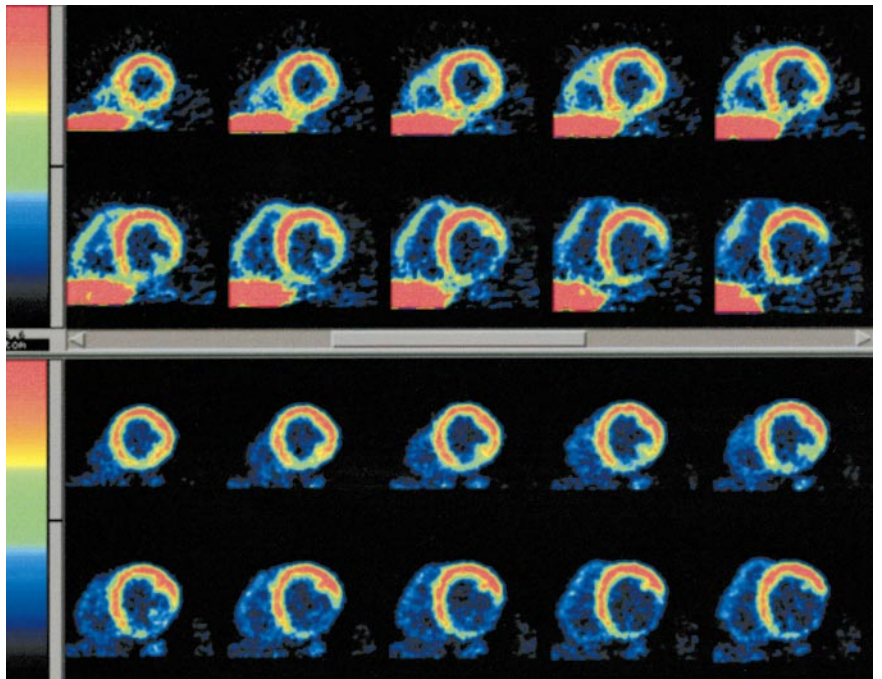


FIGURE 2. Representative short-axis reformatted summed $[^{18}\text{F}]\text{FTHA}$ (top) and FDG (bottom) images from same patient.

expected increased myocardial activity during the programmed infusion, followed by the plateau of activity after the 10-min infusion. No patient showed a decline in myocardial activity after stopping the infusion, indicating that activity in the myocardial ROI represents trapped $[^{18}\text{F}]\text{FTHA}$.

The K_i values calculated using uncorrected C_p data obtained during $[^{18}\text{F}]\text{FTHA}$ infusion showed good correlation

with K_i values calculated using HPLC-corrected C_p values (slope = 1.04 ± 0.1 , $r = 0.97$). In addition, a pooled metabolite correction function was applied to data from all 12 patients. The comparison between K_i values using this correction function and uncorrected infusion data showed excellent correlation (slope = 1.06 ± 0.07 , $r = 0.98$). Given the small error introduced by the use of the generalized function and the technical difficulty of the metabolite anal-

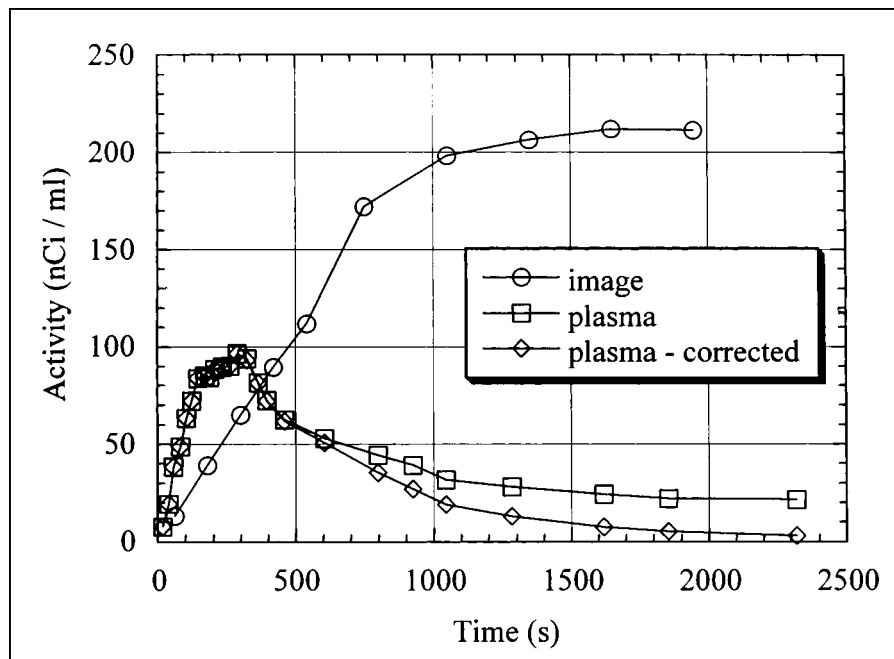


FIGURE 3. Myocardial region-of-interest activity, total plasma activity, and metabolite-corrected time-activity curves after $[^{18}\text{F}]\text{FTHA}$ infusion.

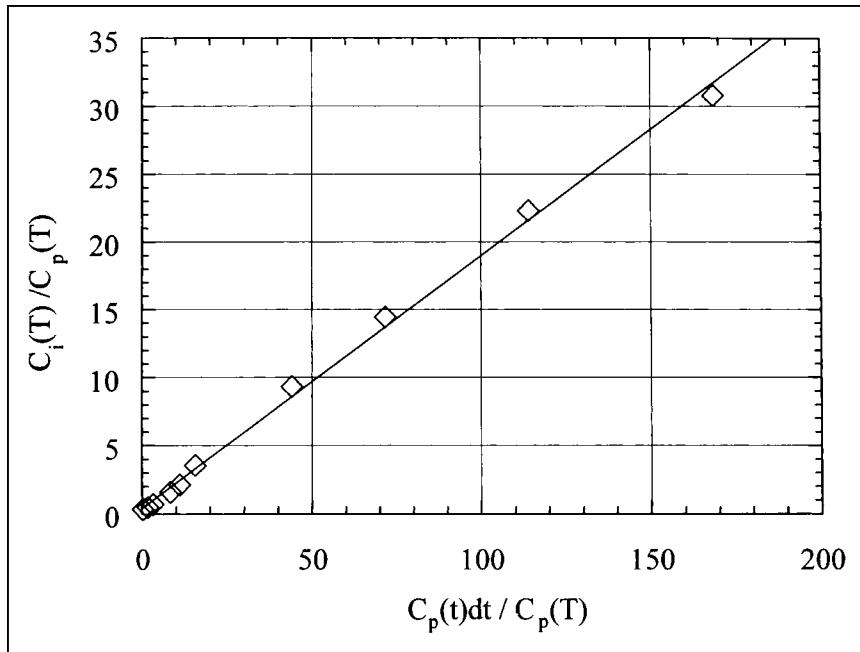


FIGURE 4. Example of graphic analysis plot for calculation of myocardial [^{18}F]FTHA uptake rate K_i .

ysis, the final K_i values were determined with uncorrected data obtained during [^{18}F]FTHA infusion.

For all patients, the graphic analysis plots were linear, indicating tracer trapping in the myocardium (Fig. 4). The average K_i for [^{18}F]FTHA was 19.7 ± 9.3 mL/100 g/min (range, 7.2–36.0 mL/100 g/min). The average fatty acid use rate was 19.3 ± 2.3 $\mu\text{mol}/100$ g/min. The K_i and fatty acid use rates for [^{18}F]FTHA in individual patients are shown in Table 3. The mean values are compared with K_i values measured in two previous studies performed on fasting human subjects using the same [^{18}F]FTHA tracer (Fig. 5A). The measured K_i in our patients was significantly greater than the K_i obtained in fasting healthy volunteers by Ebert et al. (14) (11.0 ± 2.0 mL/100 g/min, $P < 0.01$) and also significantly greater than the K_i obtained in patients with coronary artery disease and preserved left ventricular func-

tion by Maki et al. (15) (11 ± 4.0 mL/100 g/min, $P = 0.01$). The fatty acid uptake rates (Fig. 5B) were also approximately threefold higher in the current study than those reported by Maki et al. (5.8 ± 1.7 $\mu\text{mol}/100$ g/min, $P < 0.001$).

PET Images and Kinetic Analysis for FDG

Because the patients were fasting, dynamic FDG images showed little myocardial uptake. Plasma radioactivity curves for FDG showed the early peak and plateau of radioactivity after a bolus injection. The average K_i for FDG was 1.5 ± 0.37 mL/100 g/min (range, 0.1–3.3 mL/100 g/min), and the average glucose use was 12.3 ± 2.3 $\mu\text{mol}/100$ g/min. The K_i and glucose use rates for FDG in individual patients are shown in Table 3. The mean glucose uptake rate reported by Choi et al. (17)

TABLE 3
Individual Patient Uptake Rates for [^{18}F]FTHA and FDG

Patient no.	[^{18}F]FTHA K_i (mL/100 g/min)	[^{18}F]FTHA MUR ($\mu\text{mol}/100$ g/min)	FDG K_i (mL/100 g/min)	FDG MUR ($\mu\text{mol}/100$ g/min)
1	31.0	19.7	1.1	9.1
2	25.0	27.1	1.2	11.2
3	19.0	23.9	0.1	0.7
4	18.0	24.2	0.1	1.2
5	12.0	9.5	3.0	22.1
6	7.2	7.9	1.1	8.2
7	36.0	27.2	3.3	21.8
8	19.0	12.9	1.0	7.2
9	12.0	10.2	3.0	23.8
10	12.0	16.1	0.5	3.4
11	12.6	13.1	2.6	26.5
12	32.0	39.3		
Mean	19.7	19.3	1.5	12.3

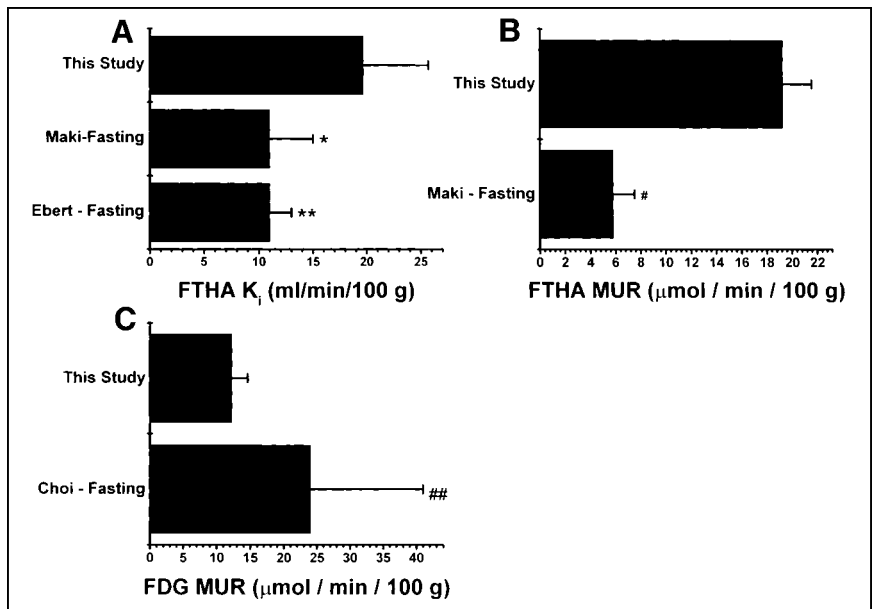


FIGURE 5. (A) Comparison of K_i values for myocardial fatty acid uptake from this study with K_i values derived from two published studies of normal human heart using [18 F]FTHA (14,15). (B) Comparison of myocardial free fatty acid uptake rates from this study with previous study using [18 F]FTHA in normal human heart (15). (C) Comparison of myocardial glucose uptake rates from this study with previous study using FDG in normal human heart (17). * $P < 0.01$; ** $P < 0.006$; # $P < 0.0005$; ## $P < 0.05$.

($24 \pm 17 \mu\text{mol}/100 \text{ g}/\text{min}$) was also twice the rate we found ($P < 0.05$; Fig. 5C).

DISCUSSION

Fatty Acid Uptake Imaging

To our knowledge, this study is the first to evaluate alterations in myocardial fatty acid use in patients with heart failure using [18 F]FTHA. Our main finding is that myocardial fatty acid uptake in nonischemic regions as measured by [18 F]FTHA in patients with heart failure is significantly higher than that found in fasting healthy volunteers in two previous studies (14,15). The previous studies showed identical mean K_i values, 11.0 mL/100 g/min, supporting the reproducibility of [18 F]FTHA-derived measurements. The mean K_i value found in our patients is significantly higher than that found by either prior study. The metabolic uptake rate for [18 F]FTHA in our study was also significantly higher than the rate calculated by Maki et al. (15) for the normal human heart. All patients had myocardial uptake rates for [18 F]FTHA that were greater than the mean myocardial uptake rates reported by Maki et al. Our findings agree with those of Paolisso et al. (18), who used indirect calorimetry to show increased myocardial fatty acid oxidation and decreased myocardial glucose oxidation in patients with heart failure.

Serum free fatty acid concentrations in our patients were also elevated and higher than concentrations reported by Maki et al. (15) ($1.01 \pm 0.08 \mu\text{mol}/\text{mL}$ versus $0.56 \pm 0.80 \mu\text{mol}/\text{mL}$). This expected finding is consistent with previous studies showing elevated serum free fatty acids in heart failure (18). This increase in serum free fatty acid concentrations could partly explain the higher calculated fatty acid metabolic uptake rates seen in our study. However, we also found an increase in the mean [18 F]FTHA uptake rate con-

stant (K_i), suggesting that fractional myocardial fatty acid uptake and use are also increased in heart failure.

The conclusions of this study depend on the biokinetics of the [18 F]FTHA tracer, a radiolabeled long-chain fatty acid analog. Initial studies showed that [18 F]FTHA is a metabolically trapped tracer (19). The rate of radioactivity accumulation of [18 F]FTHA is believed to reflect the β -oxidation rate of long-chain fatty acids. DeGrado et al. (19), using mice, showed an 87% decline in myocardial [18 F]FTHA uptake after treatment with the carnitine palmitoyl-transferase I inhibitor 2[5-(4-chlorophenyl)pentyl]oxirane-2-carboxylate, an agent known to block free fatty acid β -oxidation. Stone et al. (20) evaluated [18 F]FTHA extraction in pigs under various metabolic conditions and showed a decline in [18 F]FTHA extraction fraction that paralleled the decline in ^3H -palmitate measured β -oxidation during lactate infusion but not during hypoxia. Trapping and minimal backdiffusion of the label with [18 F]FTHA administration has allowed quantitative assessment of [18 F]FTHA tracer uptake and quantitation of β -oxidation rates in a manner similar to FDG studies for determining glucose phosphorylation rates.

[18 F]FTHA was developed to noninvasively measure alterations in myocardial substrate use. One potential use of this tracer is to evaluate the metabolic consequences of heart failure and, ultimately, to assess therapies designed to improve energy metabolism. Other PET radiotracers have previously been used for this purpose. [^{11}C]acetate, for example, has been successfully used to evaluate overall myocardial oxidative metabolism in patients with heart failure, with myocardial oxidative metabolism decreasing after the use of β -adrenergic blockade (21). The advantage of [18 F]FTHA and FDG tracers is the ability to assess changes in specific myocardial substrate use, as opposed to overall myocardial energy metabolism with [^{11}C]acetate.

Tracers have also previously been used to evaluate myocardial free fatty acid metabolism noninvasively (22). The radioiodinated fatty acid 15-(*p*-iodophenyl)-3-(*R,S*)-methyl pentadecanoic acid has been the most extensively studied; however, it may have reduced sensitivity for β -oxidation rates as a result of incorporation of tracer label into complex lipids (23). [^{13}C]palmitate has been used to evaluate fatty acid β -oxidation quantitatively using dynamic PET imaging (24) but is complicated by tracer backdiffusion and trapping of tracer in intermediary lipid pools (25).

FDG Imaging

Glucose use was expected to be low in our patients, given the known preference of the heart for fatty acid oxidation in the fasting state. Additionally, myocardial insulin resistance has been shown in heart failure (26) and correlates with the severity of heart failure independent of the presence of coronary artery disease (27). In our study, the fasting state was used to assess both fatty acid and glucose uptake rates under similar, controlled, and stable physiologic metabolic conditions. Similar to previous studies (28,29), we found a wide variation in myocardial FDG uptake, which can be explained by the low count statistics for FDG in our study and the influence of differing serum catecholamine, insulin, glucose, and fatty acid levels in our patients. The mean FDG uptake rate in our patients was significantly lower ($P < 0.05$) than reported in fasting healthy volunteers by Choi et al. (17) ($24.0 \pm 17.0 \mu\text{mol}/100 \text{ g}/\text{min}$) (Fig. 5C). Despite this variability, all patients but one had a myocardial FDG uptake rate that was lower than that found by Choi et al. (Table 3). Our results also agree with those of Paolisso et al. (18), who found glucose metabolism to be lower in heart failure patients than in healthy volunteers. As expected, glucose use is not completely abolished in heart failure, given the requirement for myocardial glucose oxidation to replenish necessary Krebs cycle intermediates (30).

Myocardial Metabolism in Heart Failure

Chronic activation of the adrenergic and renin-angiotensin systems in heart failure results in an unfavorable shift in myocardial energy metabolism and futile cycling of free fatty acids through lipolysis and reesterification, resulting in a net reduction in myocardial energy efficiency (3-5,31). Ultimately, as proposed by Katz (32), the failing heart becomes an energy-starved heart. Under normal fasting conditions, exogenous fatty acids are the preferred metabolic substrate of the heart, accounting for 60%-70% of the energy production (31). Fatty acid oxidation, however, is known to require more oxygen per unit of mechanical work performed than glucose and is therefore a less energy-efficient substrate (5,7). Fatty acid oxidation yields only 2.8 mol adenosine triphosphate per mole of nonesterified free fatty acid consumed (respiratory quotient, 0.7), compared with glucose and lactate, which yield 3.0-3.2 mol adenosine triphosphate per mole of glucose or lactate consumed (respiratory quotient, 1.0) (33). Elevation of serum catecholamines in the setting of heart failure stimulates release

and use of free fatty acids by the heart (5,7). Enhanced gene expression of several rate-limiting enzymes in fatty acid oxidation and suppressed gene expression of the rate-limiting enzyme for glucose oxidation has been shown in heart failure (4). Shifts in myocardial fatty acid and glucose use may be an important mechanism for the impaired efficiency of the failing heart and a target for specific therapies designed to improve energy efficiency and decrease overall energy requirements (3,34). The use of PET with metabolic trapped tracers, as shown in this study, is uniquely suited to assess alterations in myocardial substrate use noninvasively in humans.

Myocardial Metabolism and Contractility

Several investigators have shown a link between myocardial energy metabolism and impaired heart function. Myocardial energy efficiency in heart failure declines and is as low as 15%, whereas in healthy volunteers or patients with coronary artery disease without heart failure it is as high as 40% (35). Inhibition of fatty acid oxidation using etomoxir (an inhibitor of mitochondrial carnitine palmitoyl transferase I activity) has been shown to prevent contractile dysfunction, shift myosin heavy-chain isozyme from β - to α -myosin, and prevent deterioration in the sarcoplasmic reticulum Ca^{2+} handling (36,37). β -blockade with metoprolol has also been shown to inhibit carnitine palmitoyl transferase I activity (38) and may explain the beneficial effects of this therapy on myocardial energy metabolism (3). An improvement in myocardial efficiency has been shown using dichloroacetate to stimulate pyruvate dehydrogenase, resulting in inhibition of fatty acid oxidation and stimulation of glucose and lactate consumption by the heart (39). The improvement in energy metabolism resulting from these therapies may be an important target for therapeutic interventions in the treatment of heart failure. PET using FDG and [^{18}F]FTHA, as shown in this study, is capable of quantitatively determining the metabolic condition of the heart. These tracers can be valuable tools in the assessment of treatments designed to improve heart failure progression by affecting myocardial energy metabolism. In addition, the evaluation of the beneficial metabolic effects of therapies known to be successful in the treatment of heart failure, such as β -blockade, can help to define mechanisms for the clinical benefits of these agents.

Study Limitations

The patients recruited for this study were not a homogeneous population and included individuals with both ischemic and nonischemic cardiomyopathy. Despite these differences, the mean K_i for patients with nonischemic cardiomyopathy was similar to that for patients with ischemic cardiomyopathy (21.6 versus 19.3 mL/100 g/min). Second, regions of interest were drawn in presumably nonischemic myocardial segments. Blood flow in our patients was not evaluated, and therefore, differences in regional myocardial [^{18}F]FTHA and FDG uptake related to variations in blood flow were not assessed. Acute reductions in

myocardial blood flow precipitating myocardial ischemia can alter substrate use and may affect our results. However, this effect is unlikely to be a major factor in our study, given that patients were required to be receiving stable medical therapy for at least 3 mo before study entry and were excluded if they reported symptoms of angina. Additionally, [¹⁸F]FTHA and FDG uptake were evaluated in segments with normal contractility by echocardiography, avoiding segments that could potentially have ischemic stunning. Results from the myocardial segments we selected in our patients may not reflect overall myocardial fatty acid and glucose uptake. Third, PET studies were not performed on a control population, and this lack may affect the strength of our observations. However, two previous studies on subjects without heart failure have shown identical K_i values.

CONCLUSION

Kinetic analysis of [¹⁸F]FTHA and FDG dynamic PET images suggests that myocardial fatty acid uptake is increased and myocardial glucose uptake is decreased in patients with heart failure. These PET tracers provide a way to assess the metabolic state of cardiac myocytes in heart failure patients before and during pharmacologic interventions.

ACKNOWLEDGMENT

This study was supported by a merit review grant from the Medical Research Service of the Department of Veterans Affairs and by grant M01 RR03186 from the National Institutes of Health, Bethesda, MD.

REFERENCES

1. Thomas JA, Marks BH. Plasma norepinephrine in congestive heart failure. *Am J Cardiol*. 1978;41:233–243.
2. Haft JL. Cardiovascular injury induced by sympathetic catecholamines. *Prog Cardiovasc Dis*. 1974;17:73–85.
3. Eichhorn EJ, Hesch CN, Barnett JH, et al. Effect of metoprolol on myocardial function and energetics in patients with nonischemic dilated cardiomyopathy: a randomized, double-blind, placebo-controlled study. *J Am Coll Cardiol*. 1994;24:1310–1320.
4. Reynolds MV, Bush EW, Taft CS, Roden RA, Bristow MR. Altered gene expression of several rate-limiting enzymes in fatty acid oxidation and glycolysis in the failing human heart [abstract]. *Circulation*. 1994;90(suppl 1):I-209.
5. Kjekshus JK, Mjos OD. Effect of inhibition of lipolysis on myocardial oxygen consumption in the presence of isoproterenol. *J Clin Invest*. 1972;51:1767–1776.
6. Katz AM. Mechanisms and abnormalities of contractility and relaxation in the failing heart. *Cardiology*. 1993;38:39–43.
7. Mjos OD. Effect of free fatty acids on myocardial function and oxygen consumption in intact dogs. *J Clin Invest*. 1971;50:1386–1389.
8. Roberts AD, Daniel LC, Nickles RJ. A high power target for the production of [F-18] fluoride. *Nucl Instrum Methods Phys Res*. 1995;99:797–801.
9. DeGrado TR. Synthesis of 14(R,S)-[¹⁸F] fluoro-6-thia-heptadecanoic acid (FTHA). *J Labeled Comp Radiopharm*. 1991;29:989–995.
10. Taylor MD, Roberts AD, Nickles RJ. Improving the yield of 2-[F-18]fluoro-2-deoxyglucose (FDG) using a microwave cavity. *Nucl Med Biol*. 1996;23:605–609.
11. Patlak CS, Blasberg RS. Graphical evaluation of blood-to-brain transfer constants from multitime uptake data: generalizations. *J Cereb Blood Flow Metab*. 1985;5:584–590.
12. Ratib O, Phelps ME, Huang SC, Henze E, Selin CE, Schelbert HR. Positron tomography with deoxyglucose for estimating local myocardial glucose metabolism. *J Nucl Med*. 1982;23:577–586.
13. Pooley RA. Evaluation of 14(R,S)-[fluorine-18]fluoro-6-thia-heptadecanoic acid (FTHA) as a positron emission tomography fatty acid tracer of beta-oxidation in the heart [dissertation]. Madison, WI: University of Wisconsin; 1995.

14. Ebert A, Herzog H, Stöcklin GL, et al. Kinetics of 14 (R,S)-¹⁸F-fluoro-6-heptadecanoic acid in normal human hearts at rest, during exercise, and after dipyridamole injection. *J Nucl Med*. 1994;35:51–56.
15. Maki MT, Haaparanta M, Nuutila P, et al. Free fatty acid uptake in the myocardium and skeletal muscle using fluorine-18-fluoro-6-thia-heptadecanoic acid. *J Nucl Med*. 1998;39:1320–1327.
16. Zambon A, Hatfield B, Budinger TF. Analysis of techniques to obtain plasma for measurement of levels of free fatty acids. *J Lipid Res*. 1993;34:1021–1028.
17. Choi Y, Brunken R, Hawkins R, et al. Factors affecting myocardial 2-[F-18]fluoro-2-deoxy-D-glucose uptake in positron emission tomography studies of normal humans. *Eur J Nucl Med*. 1993;20:308–318.
18. Paolisso G, Gambardella A, Galzerano D, et al. Total-body and myocardial substrate oxidation in congestive heart failure. *Metabolism*. 1994;43:174–179.
19. DeGrado TR, Coenen HH, Stöcklin G. 14(R,S)-¹⁸F-fluoro-6-thiaheptadecanoic acid (FTHA): evaluation in mice of a new probe of myocardial utilization of long-chain fatty acids. *J Nucl Med*. 1991;32:1888–1896.
20. Stone CK, Pooley RA, DeGrado TR, et al. Myocardial uptake of the fatty acid analog 14-¹⁸F-fluoro-6-heptadecanoic acid (FTHA) in comparison to beta-oxidation rates by tritiated palmitate. *J Nucl Med*. 1998;39:1690–1696.
21. Beanlands RS, Nahmias C, Gordon E, et al. Beta blocker therapy improves cardiac efficiency in patients with left ventricular dysfunction [abstract]. *Circulation*. 1999;100:I-26.
22. Corbett J. Fatty acids for myocardial imaging. *Semin Nucl Med*. 1999;29:237–258.
23. DeGrado TR, Holden JE, Ng CK, Raffel DM, Gatley SJ. Comparison of 16-iodohexadecanoic acid (IDHA) and 15-p-iodophenylpentadecanoic acid (IPPA) metabolism and kinetics in the isolated rat heart. *Eur J Nucl Med*. 1988;15:78–80.
24. Schelbert HR, Henze F, Sochor H. Effects of substrate availability on myocardial C-11 palmitate kinetics by positron emission tomography in normal subjects and patients with ventricular dysfunction. *Am Heart J*. 1986;111:1055–1064.
25. Veerkamp JH, Van Moerkerk HTB, Glatz JFC, Zuurveld JGEM, Jacobs AEM, Wagenmakers AJM. ¹⁴CO₂ production is not adequate measure of [¹⁴C] fatty acid oxidation. *Biochem Med Metab Biol*. 1986;35:248–259.
26. Paternostro G, Camici PG, Lammertsta AA, Marinho N, Baliga RR. Cardiac and skeletal muscle insulin resistance in patients with coronary heart disease. *J Clin Invest*. 1996;98:2094–2099.
27. Swan JW, Anker S, Walton C, et al. Insulin resistance in chronic heart failure: relation to severity and etiology of heart failure. *J Am Coll Cardiol*. 1997;30:527–532.
28. Berry JJ, Baker JA, Pieper KS, Hanson MW, Hoffman JM, Coleman RE. The effect of metabolic milieu on cardiac PET imaging using fluorine-18-deoxyglucose and nitrogen-13-ammonia in normal volunteers. *J Nucl Med*. 1991;32:1518–1525.
29. Gropler RJ, Siegel AL, Moerlein SM, Perry D, Bergmann SR, Geltman EM. Nonuniformity in myocardial accumulation of fluorine-18-fluorodeoxyglucose in normal fasted humans. *J Nucl Med*. 1990;31:1749–1756.
30. Russell RR, Taegtmeier H. Pyruvate carboxylation prevents the decline in contractile function of rat hearts oxidizing acetoacetate. *J Physiol*. 1991;261:H1756–H1762.
31. Neely JR, Morgan HE. Relationship between carbohydrate and lipid metabolism and the energy balance of heart muscle. *Ann Rev Physiol*. 1974;36:413–459.
32. Katz A. Cellular mechanisms in congestive heart failure. *Am J Cardiol*. 1988;62:3A–8A.
33. Kahles H, Hellige G, Hunneman DH, Mezger VA, Bretschneider HJ. Influence of myocardial substrate utilization on oxygen consumption of the heart. *Clin Cardiol*. 1982;5:286–293.
34. Eichhorn EJ, Bedotto JB, Malloy CR, et al. Effect of beta-adrenergic blockade on myocardial function and energetics in congestive heart failure. *Circulation*. 1990;82:473–483.
35. Takaoka H, Takeuchi MT, Odake M. Comparison of hemodynamic determinants for myocardial oxygen consumption under different contractile states in human ventricle. *Circulation*. 1993;87:59–69.
36. Rupp H, Schulze W, Vetter R. Dietary medium-chain triglycerides can prevent changes in myosin and SR due to CPT-I inhibition by etomoxir. *Am J Physiol*. 1995;269:R630–R640.
37. Vetter R, Rupp H. CPT-I inhibition by etomoxir has a chamber-related action on cardiac sarcoplasmic reticulum and isomyosins. *Am J Physiol*. 1994;267:H2091–H2099.
38. Panchal AR, Stanley WC, Kerner J, Sabbah HN. Beta-receptor blockade decreases carnitine palmitoyl transferase I activity in dogs with heart failure. *J Card Fail*. 1998;4:121–126.
39. Bersin RM, Wolfe C, Kwasman M, et al. Improved hemodynamic function and mechanical efficiency in congestive heart failure with sodium dichloroacetate. *J Am Coll Cardiol*. 1994;23:1617–1624.